Journal of Structural Geology, Vol. 5, No. 5, pp. 471 to 482, 1983
Printed in Great Britain

0191–8141/83 $03.00 + 0.00
Pergamon Press Ltd.

The geometrical evolution of normal fault systems

JAMES JACKSON

and

DAN MCKENZIE

Bullard Laboratories, Madingley Rise, Madingley Road, Cambridge CB3 0EZ, U.K.

(*Received* 31 *January* 1983; *accepted in revised form* 6 *May* 1983)

Abstract—The purpose of this paper is to examine the kinematic behaviour of normal fault systems and see what general conditions govern their geometrical evolution. We pay particular attention to seismological and surface data from regions of present day active normal faulting, as the instantaneous three-dimensional geometry at the time of fault movement is better known in active regions than in areas where the faults are now static.

Most normal faults are concave upward, or listric. This shape can be produced by geometric constraints, either because the faults reactivate curved thrusts, or because they must be curved to accommodate rotations. Another effect which will produce curved faults is the variation of rheology with depth: brittle failure at shallow depths produces less fault rotation than does distributed creep in the lower part of the crust. An important geometric feature of normal faulting is the uplift of the footwall. The amount of such uplift is related not only to the elastic properties of the lithosphere, but also to the throw and dip of the fault. A striking feature of active normal faults is that they occur in groups in which all the faults dip in the same direction. This behaviour arises because the faults cannot intersect: if they do, one must cease to be active. The rotation which such fault systems produce reduces the dip of the faults until a new steeply dipping fault is formed. Once a new fault cuts pre-existing faults the earlier faults become locked, and a new set of faults must propagate rapidly across the whole region involved. Many of these geometric constraints also apply to thrust faulting.

INTRODUCTION

RECENT attention to the details of plate creation on oceanic ridges and to mechanisms of sedimentary basin formation in continental interiors has emphasized the importance of normal faults. It is therefore of interest to understand the evolution of isolated faults and the interaction of such faults with each other when they form an extensional system. The purpose of this paper is to examine the geometry of normal faults and the kinematic consequences of their movement. We have not attempted to address the more difficult question of their dynamics, and will therefore be concerned with displacements and strains, not stresses.

Although some of the ideas we discuss have been known for some time, this paper is not intended to be a comprehensive review of normal faulting, and is rather different in emphasis from most other treatments of this subject (e.g. Bally *et al.* 1981, Wernicke & Burchfiel 1982). We will be particularly concerned with constraints on fault kinematics imposed by observational data from areas of *active* present day faulting, such as the Aegean and central Greece. There are several reasons for concentrating on active regions.

(1) Most seismic faulting takes place during large earthquakes, which are comparatively rare. By studying the faulting associated with the largest earthquakes in a region we can be sure that we are dealing with the major faults responsible for the large-scale motions, and are not being misled by minor features such as the internal deformation of blocks bounded by the major normal faults.

(2) Seismological observations of the earthquake source tell us the fault orientation and slip vector (fault plane solution) at the depth of rupture initiation. This depth is typically 8–12 km in continental areas. By combining these observations with surface data we can know the fault geometry from the surface to depths of about 10 km *at the time of movement*; information that is simply not available in older, static regions where the present-day fault orientation has been affected by substantial uplift or rotation of the vertical.

(3) The seismic activity on a regional scale allows us to see the interaction between the major faults in a fault system at the time of movement. This is also difficult to deduce from static structures.

(4) A particular advantage of the Aegean is that much of it is below sea level. Ironically, although this obscures exposure, it provides a horizontal reference level against which to measure both vertical motions (uplift and subsidence) and tilt. The associated sedimentation also permits the accurate dating of structures and their associated vertical motions. As will be seen, these advantages are substantial.

Many of the ideas developed in this paper were suggested from investigations of normal faulting in central Greece, the Aegean, and western Turkey. Many faults are active in this region and their behaviour is dominated by their interaction. In particular, they can only remain active where they meet or intersect if certain conditions are fulfilled. These conditions, which are discussed in a later section, are geometric in origin and related also to the mechanical properties of rock. They are therefore general and impose kinematic constraints on both fault geometry and evolution in all areas of large-scale normal faulting where mass is conserved (but not necessarily in places like Iceland, where mass addition and dyke injection reach the surface). Because these conditions are kinematic, they apply regardless of the driving forces responsible for the normal faulting and extension. This allows us to compare structures in areas of active faulting with those in older geological terranes, or, specifically, to use features in the Aegean to guide us in the interpretation of structures in the Basin and Range Province and North Sea. All three are areas of large-scale continental extension and normal faulting, though in each case the *cause* of the extension may well have been different. As will be seen, these conditions also impose constraints on the geometry of thrust systems.

In the next (second) section, we discuss the geometry of individual normal faults. Two features of isolated normal faults which are of geological importance are footwall uplift and fault curvature. Both can be quantitatively related to the amount of extension. The third section of our paper is concerned with the interaction between faults. The second and third sections are not intended to be exhaustive reviews, and we deliberately address only what we regard as relevant to our discussion of fault kinematics. In the fourth section, we review the geometrical evolution and interaction of normal fault systems in the Aegean.

Throughout the discussion we assume that the regions between major faults form rigid blocks which cannot deform. Though aftershock locations and antithetic faulting show that this assumption is not generally valid, it does allow us to discuss kinematic problems relatively simply.

INDIVIDUAL NORMAL FAULTS

Listric faults and crustal rheology

The dip of many normal faults appears to flatten with depth. This listric geometry is often ascribed to the existence of a weak layer within the crust or sediment pile. In some cases the existence of weak layers can be demonstrated. Growth faults in the sediment piles on the northern margin of the Gulf of Mexico and in the Niger delta sole-out within layers of evaporite or overpressured shale (see e.g. Garrison & Martin 1973, Buffler *et al.* 1978). The movement on these faults is driven by gravity alone, and no plate motions are involved. On a smaller scale landslips have a similar geometry. In both these cases conservation of mass requires that the downward displacement of the material at the top of the moving body should be balanced by upward movement of the material at its bottom. Also in both cases the material beneath the fault is not deformed by its movement, and hence the displacement surface must intersect the Earth's surface at the base of the moving body as well as at its top. These conditions require growth faults and slip surfaces to be concave upward.

The same conditions do not apply to listric faults when they take up the motion at plate boundaries. There is then no requirement that the faults intersect the Earth's surface at its base, as well as at its top. In central Greece and western Turkey there is evidence that the active normal faults are approximately planar to depths of about 10 km. The most conclusive support for this claim comes from two large earthquake sequences that were studied in great detail: the 1978 series near Thessaloniki (Northern Greece) and the 1981 sequence in the eastern Gulf of Corinth. In both cases the fault plane solutions showed that the fault dips at the focii of the mainshocks were approximately 45°. Various seismological techniques were used to demonstrate that the focal depths of the mainshocks in each sequence were about 8–10 km and that the epicentres (the vertical projections of the focii to the surface) were all about 8–10 km from the surface outcrop of the faults which moved. The projections of the fault dips at the focii thus intersected the surface at the outcrop of the active faults. Although the dip of young normal faults is often very steep at the surface, this is invariably because the top few tens of metres near the Earth's surface fail in tension, not shear, commonly leaving open fissures and cracks. At Thessaloniki and Corinth, where the slip vector could be measured at the surface by matching displaced lineations such as wheel-tracks across the fissures, the dip of the slip vector at the surface agreed well with that calculated at the focal depth from seismological observations. For details of the observational data at Thessaloniki and Corinth, the reader is referred to Mercier *et al.* (1979a), Soufleris & Stewart (1981), Soufleris *et al.* (1982) and Jackson *et al.* (1982a). Thus, in these two earthquake sequences the active faults appear to have a roughly constant dip of 40–50° between the surface and a depth of about 10 km. Most, if not all, large normal faulting earthquakes in Greece and western Turkey appear to nucleate at depths of 8–12 km, and the great majority have dips of 40–50° at their focii (Jackson 1980). Although it is likely that these faults are also planar from the focal depth to the surface, only at Thessaloniki and Corinth were the necessary surface slip vector measurements and seismic observations made which allow this inference to be confirmed.

The planar nature and 40–50° dip of these active normal faults have a number of important consequences. Firstly, the dip is much steeper than the low angle dips of 0–10° that are commonly seen in the Basin and Range Province and which have received so much recent attention (e.g. Wernicke 1981, Wernicke & Burchfiel 1982, Frost & Martin 1982). In the Yerington district of western Nevada, Proffett (1977) pointed out that many of the very low angle normal faults, which are responsible for so much crustal extension, have been rotated flat by movement on later faults, and that at the time they were active had much steeper dips. He also estimated that at the time they were active, the faults in his area became horizontal only at substantial depths (16 km or more). This observation agrees well with the nature of the active normal faults in Greece: if they do flatten with depth

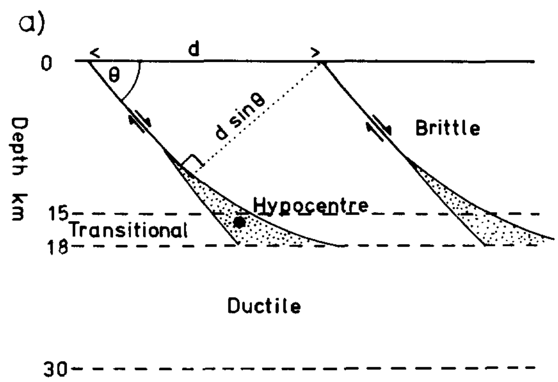

Fig. 1. (a) Sketch of the mechanical properties of the continental crust. The dotted line is perpendicular to the faults. (b) Sketch of the geometry after movement on the normal faults, used to obtain equation (1). See text for details.

they must do so below the earthquake nucleation depth of about 10 km, and any weak zone or layer within the crust must also be below this depth.

It has long been thought that the variation of crustal rheology with depth could be responsible for the listric geometry of major normal faults on the continents. We will now examine this notion quantitatively and attempt to relate it to the amount of crustal extension. The upper region of the crust fails by brittle failure, and generates seismic waves when it does so. It presumably does not have a sharp lower boundary, but merges with the underlying layer where the deformation still principally occurs on faults, but by creep rather than seismically (Sibson 1977). With increasing depth these faults cease to be slip surfaces and become slip zones (Fig. 1). Finally, if the crust is sufficiently thick, or at a high enough temperature, the lowest crustal layer creeps homogeneously and aseismically, without any discrete faults being formed. The depths at which these transitions occur must depend on the temperature gradient. Chen & Molnar (1983) used the maximum depths of continental earthquakes and Caristan's (1982) measurements on diabase to argue that the transition from seismic to aseismic behaviour occurs at a temperature of 350°C. This temperature occurs at a depth of between 10 and 15 km in many stretched basins, and it appears that most large continental earthquakes nucleate near this depth: that is, near the base of the brittle layer. Extrapolation of Caristan's experiments carried out at 1000°C suggests that the transition zone between brittle behaviour and distributed creep is less than 5 km thick in the crust, although more experiments at lower temperatures are needed before this estimate can be used with confidence. Three similar zones, of brittle, transitional and ductile behaviour, exist within the mantle, but, because the melting temperature of peridotite is greater, the temperatures of the transition regions are higher. We can now use this simplified model of crustal rheology to show that faults which are initially planar will, under most circumstances, become concave upward when the region is stretched. The geometry of the motion in the brittle seismic zone is straightforward if the faults are initially planar (Fig. 1) and rotate like a stack of books or toppling dominoes, as Ransome *et al.* (1910) and Morton & Black (1975) have proposed. It is worth noting that

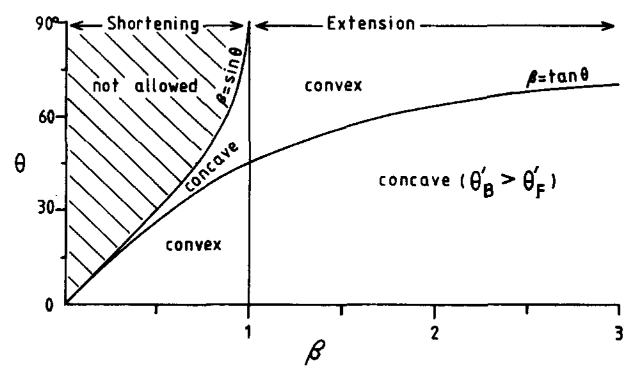

Fig. 2. Relationship between the initial dip, θ, of a planar fault, the amount of extension, β, and its dip after movement in the brittle (θ_B') and ductile (θ_F') layers. If a fault with a particular value of θ and β plots below (above) the curve it will be concave (convex) upward after deformation.

fault motion without accompanying rotation fails to produce the steep regional dips common to most extensional terranes. From Fig. 1,

$$d \sin\theta = d' \sin\theta'$$

or

$$\beta = \frac{d'}{d} = \frac{\sin\theta}{\sin\theta'},$$

where β is the amount of extension. Hence, the final dip θ_B' of the faults is related to the initial dip θ by

$$\sin\theta_B' = \frac{1}{\beta}\sin\theta. \qquad (1)$$

If the extension of the ductile layer is homogeneous it is also straightforward to determine the final inclination, θ_F', of a line drawn in the fluid at an angle θ (see Appendix 1) when the lower layer is extended by the same amount

$$\tan\theta_F' = \frac{1}{\beta^2}\tan\theta. \qquad (2)$$

Clearly, if $\theta_B' > \theta_F'$ the faults will become concave upward, whereas if $\theta_B' < \theta_F'$ the opposite geometry will be produced. It is easy to show that $\theta_B' = \theta_F'$ when

$$\beta = \tan\theta. \qquad (3)$$

Figure 2 shows the location of the line given by (3), where $\theta_B' = \theta_F'$, on a β/θ plot. When the initial dip is less

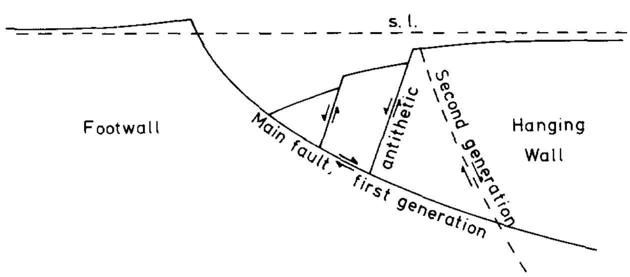

Fig. 3. Sketch of a normal fault system to show uplift of the footwall and to define the terminology used. Although the main fault is shown as a gentle curve, the arguments presented in the text suggest that, in areas where major crustal extension occurs as a result of normal faulting, a significant change in dip is likely at the brittle-ductile transition, near the base of the largest antithetic faults.

than 45° the dip of the faults in the brittle seismic zone is always steeper than the line in the ductile zone. This argument is only intended to be illustrative: it assumes that the fault is initially planar with the same dip in both brittle and ductile layers. The fault could, of course, initially be flatter in the ductile layer beneath the earthquake focal depth; in which case the arguments above will simply accentuate this initial concave geometry. Although the change in dip in the ductile layer is calculated for a line, this line may be a fault provided the slip vector always remains in the fault plane. This simple requirement is necesary to prevent the formation of voids at depth and is a fundamental and powerful constraint on fault geometry and interaction. It is discussed further in the section on interaction between faults. In this case it requires the slip vector in the ductile layer to differ from that at the surface and is one of the major causes of antithetic faulting and internal deformation in the hanging-wall block (see Fig. 3). The arguments above suggest a dramatic change in dip at the base of the brittle layer, and it is here (at a depth of 8–10 km) that movement on a large antithetic fault nucleated in the 1981 Gulf of Corinth earthquake sequence (see Jackson *et al.* 1982a). Small aftershocks, representing minor movement on small faults, typically occur throughout the hanging-wall block (Soufleris *et al.* 1982), presumably representing internal deformation caused by the change in slip vector on the main fault with depth. In practice there is likely to be a smooth change in dip between the brittle seismic region and the ductile region, producing a fault which is concave upwards. These arguments show that most faults will become listric in extensional areas, even if they start planar. The shape of the shallow part of the faults will, however, not be affected by extension, though the dip will be.

When $\beta < 1$, then the region is undergoing shortening. Under these conditions the dip of the fault will always steepen with increasing shortening, though the amount of steepening will not generally be the same in the brittle and ductile layers. Figure 2 shows that planar reverse faults which originally dipped at angles of 45° or more become concave upward. Normal faults that are buried to great depth, such as those in the stretched basement of passive continental margins, may have their original shallow planar geometry buried below the brittle–ductile transition. If they are then reactivated as thrusts (reverse faults) during subsequent compression, as Jackson (1980) suggested, their initially steep dip will cause them to evolve a concave upwards shape.

In contrast to this process, which causes a fault that is initially planar to become curved, there are various other conditions which require the faults to be concave upward initially. The most obvious is one which Wernicke & Burchfiel (1982) have discussed. Because each fault block in Fig. 1 must rotate anticlockwise through an angle $\theta_B' - \theta$ between the initial and final state, the boundary between the stretched and unstretched regions cannot be a plane fault. If it were, one side of the fault would rotate, the other would not, and a void would form. Hence the fault bounding the undeformed region must be curved, to allow one side to rotate relative to the other. The same argument applies if the amount of extension varies with position in a basin. It is also possible that the initial shape of a major extensional normal fault may be listric, though the earthquake studies discussed earlier show that such a geometry is less common than we expected.

Several authors (e.g. Kanizay 1962, Hose & Daneš 1973, Price 1977) have suggested that the curvature of normal faults is related to the stress field, and hence has a dynamic origin. They argue that the fault geometry is similar to that of slip lines within a plastic layer under vertical compression. Unfortunately, the slip lines within such a layer are not discrete surfaces on which slip is concentrated and across which there is a velocity discontinuity. In this description the velocity is continuous throughout the deforming region and cannot concentrate on faults. Hence, there is no close analogy between slip lines and faults.

In many cases it is clear that listric normal faults are produced by the reactivation of thrusts as normal faults. A good example of such behaviour is the Flathead Valley Fault in the Rocky Mountains, which Bally *et al.* (1966) showed was produced by the reversal of movement on one of the major thrusts in the area. More recently, Smythe *et al.* (1982) have proposed that the normal faults which bound the basins north of Scotland coincide at depth with pre-existing thrusts whose age is Caledonian or older. In the East Shetland Basin many large listric faults, whose geometry controls the major oil accumulations, also follow the Caledonian trend (Bowen 1975) and dip to the east. Therefore, these faults may also be reactivated Caledonian thrusts like those to the southwest. The reverse of this process has been discussed by Jackson (1980), Stoneley (1982) and Cohen (1982), who argue that listric normal faults can be reactivated as thrusts. There is no theoretical limit on the number of times the direction of motion on a fault can reverse.

The fault geometry also controls the extent to which the blocks between the faults must deform during the motion. When the faults are planar, as in Morton & Black's (1975) model and Fig. 1, their movement can be taken up without internal deformation. The rotation of the base of each faulted block is accommodated by creep

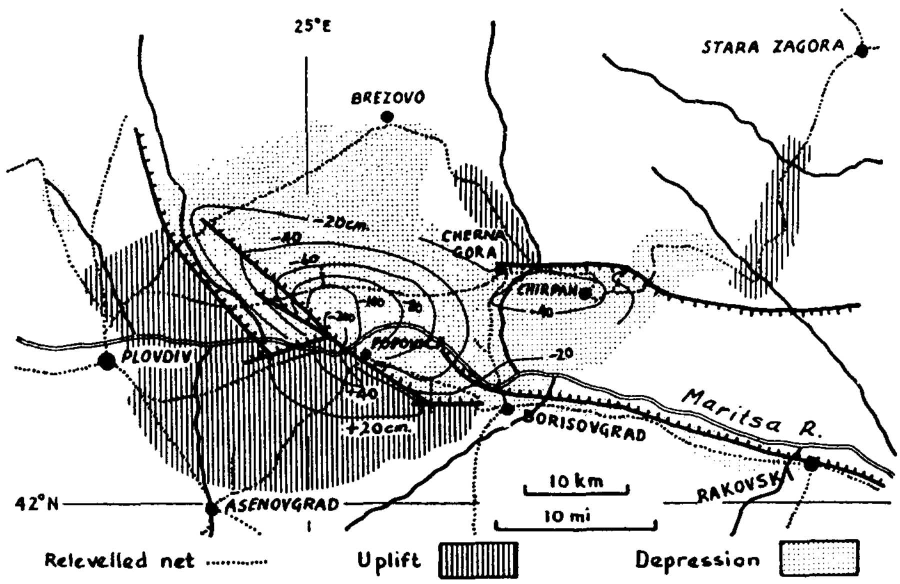

Fig. 4. Faulting and vertical movement produced by the April 1928 Bulgarian earthquakes (after Jankof 1945). Reproduced, with permission, from fig. 3.12 in *Elementary Seismology* by Charles F. Richter (W. H. Freeman & Company) © 1958.

within the crust. When, however, the faults are curved, Bally (1982) has pointed out that their movement causes the Earth's surface to become concave unless the blocks undergo internal deformation. Figure 3 shows the type of deformation required. The subsidiary faults which are required by the geometry of the motion are called antithetic faults. Movement on antithetic faults is frequently associated with earthquakes on the main faults (Myers & Hamilton 1964, Jackson *et al.* 1982a) (Fig. 4). As Proffett (1977) pointed out, continued motion on the main fault may rotate the antithetic faults past the vertical so that they appear as high-angle reverse faults.

Uplift and subsidence in normal faulting

One important feature of normal faulting which has, in our view, been insufficiently emphasized, is the uplift of the footwall. This uplift has probably helped give rise to the widespread belief that rifting is accompanied by doming. Such movement occurs for two reasons. When the fault slips during an earthquake the stress across the fault is reduced. The change in stress on the footwall is the same as that on the hanging wall, but because of their different shape the hanging wall moves down considerably further than the footwall moves up. This elastic rebound is illustrated in Fig. 4, which shows the vertical motion associated with two earthquakes in Bulgaria in 1928. This motion was determined by re-levelling soon after the earthquake and was described by Jankhof (1945) and summarised by Richter (1958). As in the 1981 Corinth earthquakes discussed by Jackson *et al.* (1982a), there were two fault breaks: a southern fault, which is probably the main fault, and a northern fault which is probably an antithetic fault. Although there is minor uplift in the footwall of the antithetic fault, there is net subsidence of the whole hanging-wall block as it slides down the main normal fault dipping north (see Fig. 3). This gives rise to the strong asymmetry in the uplift and subsidence shown in Fig. 4. The relative displacements illustrated in Fig. 4 were presumably elastic, and will be reversed (i.e. the footwall near the fault will subside relative to the footwall farther from the fault) as continued extension restores the stress to its value before the event.

There is, however, a different mechanism by which long-term uplift can be produced, which was discussed by Vening Meinesz (1950) (see Heiskanen & Vening Meinesz 1958). We use their model to estimate the ratio of the uplift to the downdrop in Appendix 2. As the hanging wall slides down the fault it unloads the footwall which is then uplifted by isostasy. The hanging wall correspondingly sinks. If the fault is completely buried beneath uniform sediment, the upward movement of the footwall is similar in magnitude to the downward movement of the hanging wall. In this case, because of the absence of a horizontal reference level, the displacements are difficult to measure. The only case where the uplift is easily measured is when the footwall is exposed above the sea surface and the hanging wall is beneath the water, where the sedimentation rate is usually sufficiently fast to fill the depression caused by faulting. The elevation of the footwall is then about one tenth of the subsidence of the hanging wall (Appendix 2) and can be determined from the topography or stratigraphy. Though the general form of the vertical motion in this case is similar to the elastic rebound, the detailed geometry is different. In particular, the movements are permanent and are not reversed by the accumulation of elastic strain. Figure 5 shows an example of permanent uplift produced by movement on a fault in the North Sea (Linsley *et al.* 1980). The uplift which forms the trap of the Beatrice oil field was produced by the unloading of a normal fault. Because the displacement on the fault has a maximum, and decreases both to the east and the west, the uplift also dies away along strike. In the southeastern direction, the structure is closed by the downthrown

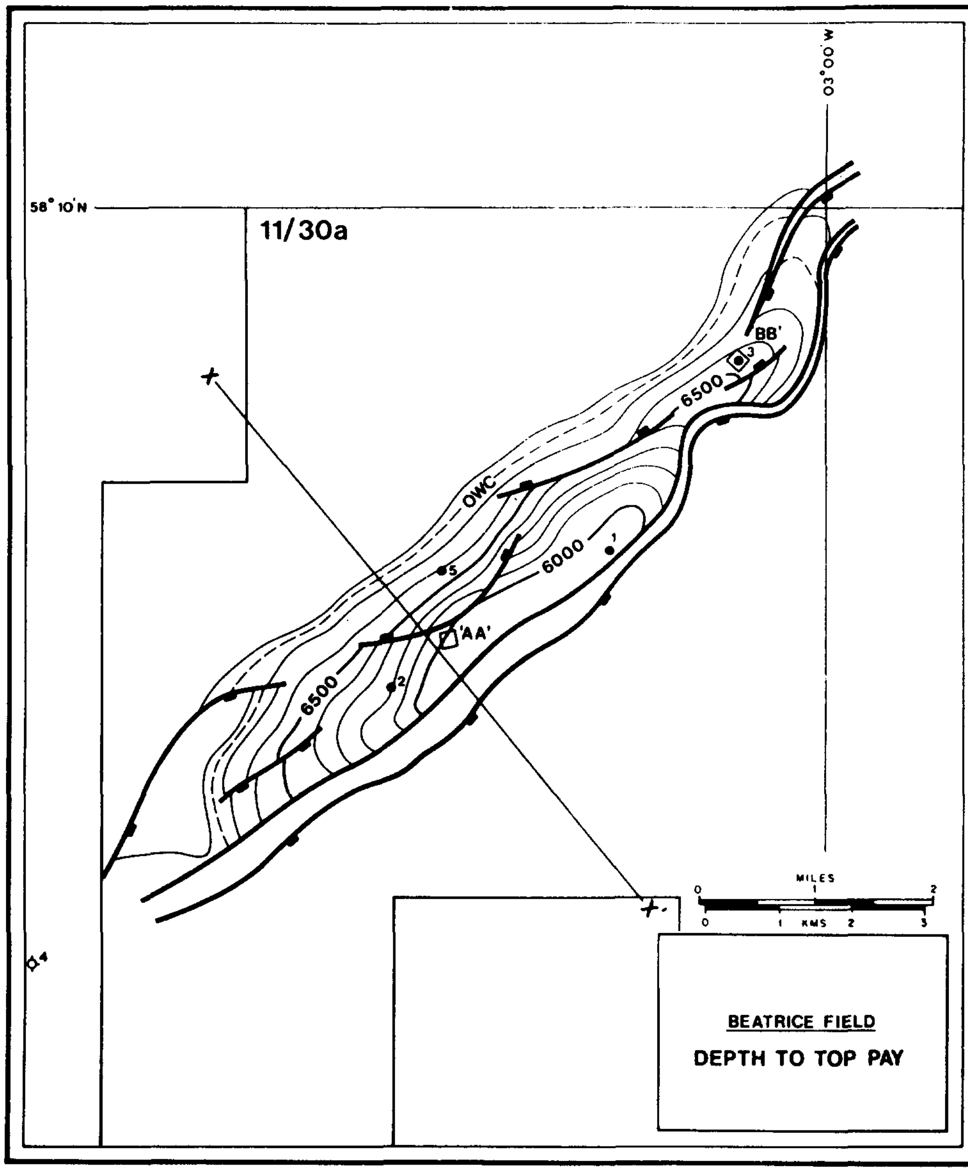

Fig. 5. Depth (in feet) to the upper surface of the reservoir of the Beatrice Field, North Sea. The heavy lines are normal faults, with rectangles on the downthrown side. Reproduced from Linsley *et al.* (1980), with permission of the author and the American Association of Petroleum Geologists.

shales, and in the northwestern direction by the decay of the uplift with increasing distance from the fault. Hence, the uplift associated with the normal fault produces closure in all four directions to form a structural trap. Progressive sediment onlap in the footwall may also give rise to potential stratigraphic traps. Exactly the same arguments can be used to estimate the uplift of the hanging wall which results from thrusting (Appendix 2).

An important feature of normal fault systems is their tendency to form new generations of high-angle faults when the dip of the original faults has been reduced by the rotation associated with their movement. New high-angle faults are required because the contribution which gravity can make to overcoming the friction on the fault plane is reduced as the dip of the fault decreases. The geometry of this process has been discussed by Morton & Black (1975) and Proffett (1977) but is rarely apparent on seismic reflection profiles. Only one generation of

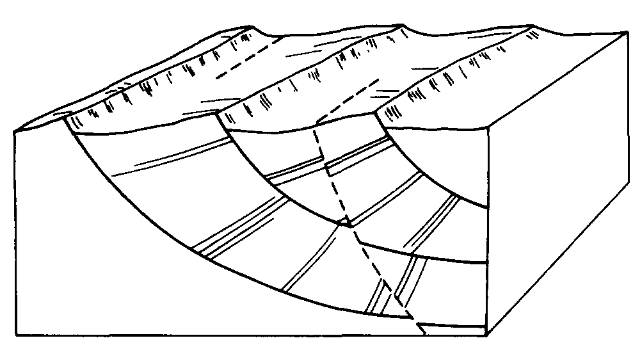

Fig. 6. Block diagram to show the interaction between the first generation of normal faults, shown by heavy lines, and the second generation, shown dashed. Movement on the second-generation fault seen on the front face of the block will lock that of the two faults it intersects. Its propagation into the plane of the page can produce another fault en échelon with the first, shown by the dashed line on the surface. Although the first-generation faults are shown with a listric geometry, they could be planar as long as the faulting extends further to the left of the block.

faults can be seen on the profiles published by Effimoff & Pinezich (1981) and de Charpal *et al.* (1978), perhaps because the stacking used during data reduction is designed to emphasize sub-horizontal strata, not those tilted at steep angles. Unlike these authors, Proffett (1977) used cores from closely spaced drill holes to interpret the structures in the Yerington area. A common, but not universal, feature of younger, steeper faults is that they cut the hanging wall (Fig. 6). This geometry has the important consequence of uplifting the sediments which were deposited close to the earlier fault and which have therefore been tilted through the greatest angles. There are two obvious explanations of this tendency. Antithetic faults of the first generation can be rotated until they dip in the same direction as the main faults, when they become planes of weakness which the second generation can exploit by reversing their displacements. Another explanation is that the second-generation faults exploit part of the fault plane of the first generation. This geometry could allow both generations to continue to move for a limited time. Angelier & Colletta (1983) suggest that vertical tension gashes, present as internal deformation within hanging-wall blocks, may grow to become later steep faults with significant displacement. Although commonly seen at the surface, these cracks can only be present as tensional fissures to the relatively shallow depths at which void formation is permissible (<500 m; see fourth section of this paper). Thus, although they may be exploited as planes of weakness near the surface, they cannot account for steep second-generation faulting at depth.

INTERACTION BETWEEN SEVERAL FAULTS

The principal constraint imposed by the existence of several faults in an area, all of which are active, is that they must not intersect. If they do cross, movement on one fault, A, will offset the other, B, whose slip vector will then no longer lie in the plane of the fault. If B were then to move a void would form. The stress drops involved in earthquakes are typically in the range 10–100 bars (see e.g. Kanamori & Anderson 1975). Only within about 500 m of the surface are these stresses sufficiently large to overcome the lithostatic pressure and form voids. As we have noted already, this inability to form voids at depth is a powerful constraint on the evolution of fault geometry. The only circumstance in which active faults can cross and both remain active is when the slip vector of one fault lies in the plane of both faults. An example of such a system, illustrated by Bally (1982), is a vertical strike–slip fault offsetting a listric normal fault. If the fault system in Fig. 3 is crossed by a vertical strike–slip fault at right angles to the strike of the normal fault and in the plane of the paper, the slip vectors on both the main and the antithetic faults lie in the plane of the strike–slip fault. Hence, their motion will not offset the strike–slip fault and all faults can continue to move. Notice that the same is not true of a strike–slip fault whose dip is not vertical. The general requirement that most active faults do not cross, and that when they do so, one ceases to be active, controls the geometry of active fault systems. An obvious consequence of this, emphasized by many authors including Bally (1982), Proffett (1977) and Stewart (1980) is that normal faults dip in the same direction over large regions. By doing so they can avoid crossing. Similarly the antithetic faults must not cross the main fault, and so most grabens are asymmetric at depth. Exactly the same rules apply to systems of thrust faults. They also must not cross each other if they are to remain active. Like normal faults, their motion is not affected if they are crossed by a vertical strike–slip fault, provided the slip vectors on the thrusts lie in the plane of the strike–slip fault.

One important consequence of these rules governing the simultaneous activity of several faults is that the initiation of a steep second generation fault can completely change the geometry of the fault movements. If the first-generation faults depicted in Fig. 6 are sufficiently closely spaced, one steep second-generation fault can lock more than one earlier fault. The first steep new fault will presumably start where the rotation of the earlier ones has been greatest, and it will lock all the earlier faults which it intersects. Hence, the new fault must take up the motion of these older faults. It will therefore rapidly propagate along its strike, in the same way as a tear or dislocation does, by concentrating the stress at its tip. If the propagating tip encounters a hard region, another new fault will be formed en échelon with the first (Fig. 6). En échelon propagation of this type, combined with footwall uplift, can produce the type of structure shown in Fig. 5. Another mechanism which can produce the same effect is the propagation of two different sets of second-generation faults into an area, each of which originated in a place remote from the other. Movement on the new faults will rapidly lock the older faults over a wide area. Once this has happened a series of second-generation faults which do not cross each other will form to take up the motion. Such behaviour will only occur if, at least somewhere in the region, the steep new faults cross more than one old fault. Otherwise the faults will move independently.

This type of interaction between faults may be the cause of the regular variation in the direction of fault dip reported from the Basin and Range Province by Stewart (1980). He remarked that the steep second-generation faults bounding the present basins and ranges dip in the same direction over large regions, and are often separated from regions with faults dipping in the opposite direction by discontinuities parallel to the slip vector. As discussed at the beginning of this section, this is the only geometry which allows all faults to move together. Zoback *et al.* (1981) pointed out that the steep second-generation faults cut through the earlier faults at the same time over large regions, which is also in agreement with the idea that they lock the first-generation faults and propagate rapidly. However, propagation along strike will be interrupted by the strike–slip faults, hence each large region in which the faults have the same dip

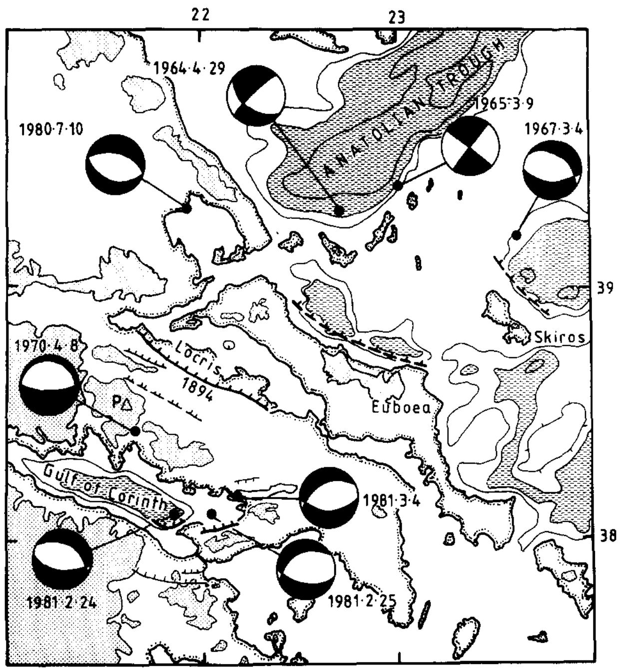

Fig. 7. Map of central Greece showing fault plane solutions (from Jackson *et al.* 1982b), bathymetry (from Morelli *et al.* 1975), and topography (from ONC chart G3). Bathymetric contours are at 400, 600 and 1000 m and shaded with horizontal lines beneath 600 m. Topography higher than 615 m is stippled. Epicentres are those reported by NOAA and its successors, except for those in the Gulf of Corinth, which are from Jackson *et al.* (1982a). Fault plane solutions are lower-hemisphere projections, with compressional quadrants shown in black. Northward-dipping normal faults that are known to have moved at the surface during earthquakes are marked by thick lines with teeth on the downthrown side. Those north of Euboea and Skiros are conjectural, based on observations of uplift and seismicity (see text). Older faults, active in the Pliocene, are marked by thinner lines in Locris and south of Corinth. The fault marked north of Mt. Parnassus (P) is based on topography and is of unknown age. The faulting marked on this map is not complete and should not be used in seismic risk assessment: it is designed to illustrate the presence of at least four sub-parallel asymmetric grabens bounded by major normal faults dipping northeast. In particular, many large southward-dipping antithetic faults are present in northwest Euboea and on the northern side of the Gulf of Corinth; only the antithetic fault which moved in the earthquake of 1981.3.4 is marked on this map.

direction should behave independently. The observations of Stewart (1980) and Zoback *et al.* (1981) would only be expected if the faults of each system are all active at the same time. The clear expression of many of the faults in the topography also suggests that many are now active (Wallace 1977, 1978), although the level of seismicity is much weaker than in the Aegean. The Basin and Range Province has probably been stretched by about a factor of two (Hamilton & Myers 1966, Proffett 1977, Priestley & Brune 1978), though the amount of extension at any particular location is variable. In this respect it is similar to the Aegean, where measurements of crustal thickness suggest similar amounts of extension in the areas which have been most strongly stretched (Makris 1976, Makris & Vees 1977, McKenzie 1978). Hence the degree of deformation in the two areas is also likely to have been similar. It is important to note that none of the arguments in this or the preceding section is affected by the nature of the driving forces responsible for the crustal extension, which may well be different in the Aegean and Basin and Range. It is because the constraint on the fault kinematics are geometric that the evolution of fault systems in the two areas can be compared.

THE AEGEAN SEA AND CENTRAL GREECE

These is no region of the Earth's surface which is well enough known to test all the proposals in the two preceding sections. Though many sedimentary basins have been investigated using reflection seismology, in most cases little is known about the detailed history of the underlying faults. Two areas which are presently being deformed by normal faults are the Aegean Sea in Greece and the Basin and Range Province in the western U.S.A. Though the geology of the second is better known, the first is much more seismically active. In particular, studies of the 1978 Thessaloniki and 1981 Gulf of Corinth earthquakes and their aftershocks have demonstrated the present relationship between surface faulting and that at depths of about 10 km (see second section). Also, enough is known of the post-Miocene history of the area to illustrate some of the processes involved. Another major advantage of the Aegean is that large parts are covered with sea water, which forms a convenient horizontal reference surface (Jackson *et al.* 1982a). We will therefore attempt to relate some of the features in the Aegean to the ideas discussed above. Too little is yet known about the instantaneous motions in three dimensions and their evolution in time for such a comparison to provide a detailed test of our suggestions. Nonetheless, the kinematic ideas outlined in the preceding sections provide a useful framework within which to discuss the observations.

The area of central Greece shown in Fig. 7 has been shaken by a number of recent large earthquakes, three of which had surface breaks. Of these the most carefully studied was the event in 1981 at the eastern end of the Gulf of Corinth (Jackson *et al.* 1982a). Vertical movement of the coast was clearly visible, and corresponded well to the motion expected from elastic rebound. Furthermore the topography of the epicentral region is clearly controlled by faulting, with the footwall probably uplifted by between 0.5 and 1 km. The argument presented in Appendix 2 suggests that the total fault displacement may be between 5 and 10 km. As Jackson *et al.* (1982b) have pointed out, many islands in the Aegean are the uplifted footwalls of major normal faults, and their elevation may also provide a simple guide to the fault displacements. Another earthquake shook the western Gulf of Corinth on 1861.12.26 (see Richter 1958). This event was associated with a surface break on the south shore of the Gulf, similar to that of the 1981 sequence, with the north side moving down. The existence of major faults and uplifted Plio-Quaternary sediments on the southern side of the Gulf suggests that the active faults at the eastern end, which have dips of 40–50° in the brittle layer, are steep second-generation faults. Jackson *et al.* (1982a) believed that the 1981.3.4 event occurred on an antithetic fault, and the 1970.4.8 shock may well have done so too, since one of the nodal planes of its fault plane solution dips steeply to the south.

Another large event took place in Locris on 1894.4.27 and was also accompanied by a surface break (Richter 1958). The footwall of this active fault contains Plio-Quaternary sediments which have been strongly tilted (Philip 1976) and large normal faults that did not move during the earthquake; again suggesting the active fault is a second-generation fault. The existence of uplifted marine terraces on northeast Euboea (Lemeille 1977), and of closed basins to the northeast of the island, together with the presence of the island itself, suggests that another major fault exists offshore, also dipping northeast. The bathymetry and seismicity of the escarpment northeast of Skiros (Fig. 7) makes it likely that this too is an active normal fault. Similar features on land suggest that another fault separates Mount Parnasos from the basins immediately north of it. The spacing between each of these faults is between 30 and 40 km; very similar to those of the Basin and Range. All of them dip to the northeast, have total lengths of about 100 km (though perhaps made up of individual segments 15–20 km long), and are likely to have throws of at least 5 km. The scale of the fault system is very large. The northwestern boundaries of all the faults lie on the prolongation of the Anatolian Trough, which is at right angles to the strike of the normal faults and which is known to have a large strike–slip component of motion from fault plane solutions (Jackson *et al.* 1982b). However, no western extension of this trough is known on land which could form this northwestern boundary. All these normal faults are sub-parallel to the major thrusts of the Hellenides (Auboin 1965). It is therefore possible that they share the same faults at depth and that the present motions are simply produced by reversing the sense of movement on the deeper thrusts, as apparently occurred in the basins north of Scotland (Smythe *et al.* 1982). However, in the absence of deep seismic reflection data this remains merely plausible in central Greece.

The geometry of the active normal faults suggests that no tectonic basement can exist anywhere in the area, and that the subsurface movements must resemble those shown in Fig. 6. Major earthquakes at Corinth in 1981 and Thessaloniki in 1978 all had depths and locations known with sufficient accuracy to show (second section of this paper) that the faults are approximately planar to a depth of about 8–10 km and dip at about 45°. This observation, the existence of tilted Plio-Quaternary rocks in the footwall of the 1894 Locris fault (Philip 1976, Mercier *et al.* 1979b), and the occurrence of normal faults in the uplifted footwalls of the active Corinth and Locris faults, as well as that northeast of Euboea, suggests that the active faults are steep second-generation faults. Their movement must have reduced or stopped the motion on the older systems in their footwalls. If the geometry of the earlier faults resembled those shown in Fig. 6, the second generation, once initiated, would have rapidly propagated throughout the area. This propagation need not, however, cross any strike–slip faults parallel to the extension direction.

The sequence of events outlined above can explain a surviving enigma in the Pliocene–Quaternary history of the Aegean. Careful structural and paleogeographical work on Neogene and Quaternary sediments in and around the Aegean led several people (e.g. Mercier *et al.* 1979b, Mercier 1981) to suggest that the normal faulting which began in central Aegean in the middle or late Miocene was interrupted by a short period of regional compression, lasting only about one million years, in the earliest Quaternary. As Jackson *et al.* (1982b) point out, some of the observations leading to this suggestion, particularly the widespread uplift seen in the islands and coastal areas of the central Aegean at the base of the Quaternary (Keraudren & Mercier 1977, Keraudren 1979), are more likely to be an artefact of renewed normal faulting. The question remains: why was the footwall uplift seen in the islands and coastal regions apparently synchronous over the whole central Aegean region? The rapid propagation of steep second-generation faults over the area in the early Quaternary appears to provide the answer. If this is so, then the earlier, now flatter, faults are presumably responsible for most of the extension in the brittle layer, whereas the steeper, new, and now active faults are responsible for the present day topography and bathymetry, as steep faults produce more footwall uplift than flatter faults (see Appendix 2).

It is not yet clear how common fault geometries like those shown in Figs. 6 and 7 are. An essential feature is that many faults must be simultaneously active, otherwise the kinematic constraints do not apply. The regional tilt patterns (Stewart 1980) and the distributed seismicity in the Basin and Range suggest that many of the range-bounding faults are now active, and that this area is deforming in the same way as the Aegean. In western Nevada, Proffett (1977) describes a sequence of events in which most of the crustal extension was achieved in the middle Miocene by faults that are now rotated to a low angle of dip and are inactive. This was followed in the late Miocene by the creation of the present-day Basin and Range topography by high-angle faulting which cuts the older faults. However, in the Basin and Range, large earthquakes with surface breaks are much less frequent than they are in the Aegean, and it is not straightforward to demonstrate simultaneous activity by any other method. One other region where a similar system of normal faults may now be active is western Turkey. The known active graben systems in the area are discussed by McKenzie (1978), but unfortunately the earthquake locations in the area are not yet accurate enough to demonstrate the geometry of the subsurface motions. It is, however, already clear that these must be more complicated than those in central Greece.

CONCLUSIONS

Continental deformation involves simultaneous movement on a variety of different faults, some planar and some curved. For the reasons discussed in the second section of this paper it is probable that faults in extensional or compressional environments become curved at depth as the deformation progresses, even if they were planar to start with. Though both types can become concave upward or downward, normal faults with dips of 45° should become concave upward. The constraint that no voids should form during the motion of the faults imposes severe constraints on the geometry of fault systems and on their evolution. Only vertical strike–slip faults are likely to cut systems of normal faults, and all such systems must contain faults dipping in the same direction. When faults of a new system, with a steeper dip, cross more than one fault of an earlier system, the new system must propagate rapidly throughout the deforming area because it prevents the first generation of faults from moving. Motion of either the new or old generation of faults will uplift the footwalls of faults, and such uplift has generated the present islands in the Aegean. The same process produced the islands on the flanks of the North Sea grabens during Cretaceous and Jurassic rift development (Wood 1982). In the uplifted footwalls of second-generation faults strongly rotated sediments deposited during the first-generation faulting may occur.

One of the most important features of the normal fault system in Greece is the horizontal scale of the faults. Most of central Greece is probably underlain by at least one normal fault. Under such conditions the labels autochthon and allochthon become meaningless. These labels remained in use after plate tectonics became accepted because many geologists believed that much continental deformation consisted of thin sheets of deforming material travelling over essentially intact lithosphere. If normal faults frequently underlie each other, are active at the same time, and chop up the whole lithosphere, the distinction between the two terms is not useful. In areas such as central Greece the terms should be redefined or abandoned.

Acknowledgements—This work would not have been possible without the detailed studies of major earthquakes which have been carried out by Geof King, Christos Soufleris, Manuel Berberian, Graham Yielding and a number of other colleagues. We realized the need for a detailed explanation of these ideas during discussions with Frank Richter and later on a field trip in western Turkey with Celal Şengör, to whom we are particularly grateful for his generous hospitality both during the trip and afterwards at Bursa, where this paper was written. We thank Graham Yielding, Peter Molnar and Jon Brewer for helpful comments on the manuscript. This work was supported by a grant from the Natural Environmental Research Council, and is contribution number 383 of Cambridge University Department of Earth Sciences.

REFERENCES

Angelier, J. & Colletta, B. 1983. Tensional fractures and extensional tectonics. *Nature, Lond.* **301**, 49–51.

Auboin, J. 1965. *Geosynclines*. Elsevier, Amsterdam.

Bally, A. W. 1982. Musings over sedimentary basin evolution. *Phil. Trans. R. Soc.* **A305**, 325–328.

Bally, A. W., Gordy, P. L. & Stewart, G. A. 1966. Structure, seismic data and orogenic evolution of the southern Canadian Rocky Mountains. *Bull. Can. Petrol. Geol.* **14**, 337–381.

Bally, A. W., Bernoulli, D., Davis, G. A. & Montadert, L. 1981. Listric normal faults. *Oceanol. Acta*, Proc. 26th Int. Geol. Cong. Geology of Continental Margins Symposium, Paris, 87–101.

Bowen, J. M. 1975. The Brent Oil Field. In: *Petroleum and the Continental Shelf of Northwest Europe* (edited by Woodland, A. W.). Applied Science Publishers, 353–362.

Buffler, R. T., Shaub, F. J., Watkins, J. S. & Worzel, J. L. 1978. Anatomy of the Mexican Ridges, southwestern Gulf of Mexico. *Mem. Am. Ass. Petrol. Geol.* **29**, 319–327.

Caristan, Y. 1982. The transition from high-temperature creep to fracture in Maryland diabase. *J. geophys. Res.* **87**, 6781–6790.

de Charpal, O., Guennoc, P., Montadert, L. & Roberts, D. G. 1978. Rifting, crustal attenuation and subsidence in the Bay of Biscay. *Nature, Lond.* **275**, 706–711.

Chen, W-P. & Molnar, P. 1983. The depth distribution of intracontinental and intraplate earthquakes and its implications for the thermal and mechanical properties of the lithosphere. *J. geophys. Res.* **88**, 4183–4214.

Cohen, C. 1982. Model for a passive to active continental margin transition: implications for hydrocarbon exploration. *Bull. Am. Ass. Petrol. Geol.* **66**, 708–718.

Effimoff, I. & Pinezich, A. R. 1981. Tertiary structural development of selected valleys based on seismic data: Basin and Range Province, northeastern Nevada. *Phil. Trans. R. Soc.* **A300**, 435–442.

Frost, E. G. & Martin, D. L. (Eds.) 1982. Mesozoic–Cenozoic evolution of the Colorado River region, California, Arizona and Utah. Cordilleran Publishers, San Diego, California.

Garrison, L. E. & Martin, R. G. 1973. Geologic structures in the Gulf of Mexico basin. *Prof. Pap. U. S. geol. Surv.* **773**, 1–85.

Hamilton, W. & Myers, W. B. 1966. Cenozoic tectonics of the western United States. *Rev. Geophys.* **4**, 509–549.

Heiskanen, W. A. & Vening Meinesz, F. A. 1958. *The Earth and its Gravity Field*, McGraw-Hill New York.

Hose, R. K. & Daneš, Z. F. 1973. Development of the late Mesozoic to early Cretaceous structures of the Great Basin. In: *Gravity Tectonics* (edited by De Jong, K. A. & Scholten, R.). John Wiley & Sons, New York, 429–441.

Jackson, J. A. 1980. Reactivation of basement faults and crustal shortening in orogenic belts. *Nature, Lond.* **283**, 343–346.

Jackson, J. A., Gagnepain, J., Houseman, G., King, G. C. P., Papadimitriou, P., Soufleris, C. & Virieux, J. 1982a. Seismicity, normal faulting and the geomorphological development of the Gulf of Corinth (Greece): the Corinth earthquakes of February and March 1981. *Earth Planet. Sci. Lett.* **57**, 377–397.

Jackson, J. A., King, G. & Vita-Finzi, C. 1982b. The neotectonics of the Aegean: an alternative view. *Earth Planet. Sci. Lett.* **61**, 303–318.

Jankhof, K. 1945. Changes in ground level produced by the earthquakes of April 14 to 18 1928 in southern Bulgaria. In: *Tremblements de Terre en Bulgarie*, Nos. 29–31, Institut meteorologique central de Bulgarie, Sofia, 131–136 (in Bulgarian).

Kanamori, H. & Anderson, D. L. 1975. Theoretical basis of some empirical relations in seismology. *Bull. seism. Soc. Am.* **65**, 1073–1095.

Kanizay, S. P. 1962. Mohr's theory of strength and Prandtl's compressed cell in relation to vertical tectonics. *Prof. Pap. U.S. geol. Surv.* **B414**, B1–16.

Keraudren, B. 1979. Le Plio-Pleistocene marin et oligihalin en Grèce: stratigraphie et paleogeographie. *Revue Géogr. phys. Géol. dyn.* **21**, 17–28.

Keraudren, B. & Mercier, J-L. 1977. Palaogeographie Plio-Pleistocene et néotectonique de l'arc Egéen. Recherches Francais sur le Quaternaire, INQUA 1977. Supplement au Bulletin AFEQ, **50**, 135–140.

Lemeille, F. 1977. Etudes néotectoniques en Grèce Centrale nord-occidentale et dans les Sporades du Nord. Thèse de 3ème cycle, University de Paris.

Linsley, P. N., Potter, H. C., McNab, G. & Racher, D. 1980. The Beatrice Field, Inner Moray Firth, U.K. North Sea. In: *Giant Oil and Gas Fields of the Decade* 1968–1978 (edited by Halbouty, M. T.). American Association Petroleum Geologists, 117–129.

Makris, J. 1976. A dynamic model of the Hellenic Arc deduced from geophysical data. *Tectonophysics* **36**, 339–346.

Makris, J. & Vees, R. 1977. Crustal structure of the central Aegean Sea and the islands of Evia and Crete, Greece, obtained by refraction seismic experiments. *J. geophys. Res.* **42**, 329–341.

McKenzie, D. P. 1978. Active tectonics of the Alpine–Himalayan belt: the Aegean Sea and surrounding regions. *Geophys. J. R. astr. Soc.* **55**, 217–254.

Mercier, J-L., Mouyaris, N., Simeakis, C., Roundoyannis, T. & Angelidhis, C. 1979a. Intraplate deformation: a quantitative study

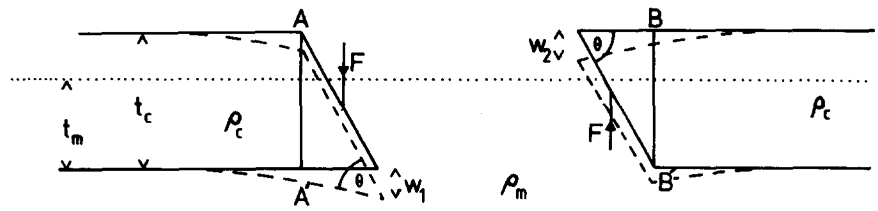

Fig. 8. Continental crust, cut by a planar normal fault, is shown separated at a fault. The constants are defined in Appendix 2. The dotted line shows the level that the fluid of density ρ_m, in which the crustal blocks are floating, would reach.

of the faults activated by the 1978 Thessaloniki earthquakes. *Nature, Lond.* **278**, 45–48.

Mercier, J.-L., Delibassis, N., Gauthier, A., Jarrige, J., Lemeille, F., Philip, H., Sebrier, M. & Sorel, D. 1979b. La néotectonique de l'arc Egéen. *Revue Géogr. phys. Géol. dyn.* **21**, 67–92.

Mercier, J.-L. 1981. Extensional-compressional tectonics associated with the Aegean arc: comparison with the Andean cordillera of south Peru–north Bolivia. *Phil. Trans. R. Soc.* **A300**, 337–355.

Morelli, C., Gantar, C. & Pisani, M. 1975. Geophysical studies in the Aegean Sea and eastern Mediterranean. *Boll. Geof. Teor. e appl.* **17**, 66.

Morton, W. H. & Black, R. 1975. Crustal attenuation in Afar. In: *Afar Depression of Ethiopia* (edited by Pilger, A. & Rösler, A.). Inter-Union Commission on Geodynamics, Sci. Rep. No. 14. E. Schweizerbart'sche Verlagsbuchhandlung, Stuttgart, 55–65.

Myers, W. B. & Hamilton, W. 1964. Deformation accompanying the Hebgen Lake earthquake of August 17, 1959. *Prof. Pap. U.S. geol. Surv.* **435**, 55–98.

Philip, H. 1976. Un épisode de déformation en compression à la base du Quaternaire en Grèce centrale (Locride et Eubée nord-occidentale) *Bull. Soc. géol. Fr.* **18**, 287–292.

Price, N. J. 1977. Aspects of gravity tectonics and the development of listric faults. *J. geol. Soc. Lond.* **133**, 311–327.

Priestley, K. & Brune, J. 1978. Surface waves and the structure of the Great Basin of Nevada and western Utah. *J. geophys. Res.* **83**, 2265–2272.

Proffett, J. M. 1977. Cenozoic geology of the Yerington district, Nevada, and implications for the nature of Basin and range faulting. *Bull. geol. Soc. Am.* **88**, 247–266.

Ramsay, J. G. 1967. *Folding and Fracturing of Rocks.* McGraw-Hill, New York.

Ransome, F. L., Emmons, W. H. & Garrey, G. H. 1910. Geology and ore deposits of the Bullfrog district, Nevada. *Bull. U.S. geol. Surv.* **407**.

Richter, C. F. 1958. *Elementary Seismology*, W. H. Freeman, San Francisco.

Sibson, R. H. 1977. Fault rocks and fault mechanisms. *J. geol. Soc. Lond.* **133**, 191–213.

Smythe, D. K., Dobinson, A., McQuillan, R., Brewer, J. A., Matthews, D. H., Blundell, D. J. & Kelk, B. 1982. Deep structure of the Scottish Caledonides revealed by the MOIST reflection profile. *Nature, Lond.* **299**, 338–340.

Soufleris, C. & Stewart, G. S. 1981. A source study of the Thessaloniki (northern Greece) earthquake sequence. *Geophys. J. R. astr. Soc.* **67**, 343–358.

Soufleris, C., Jackson, J. A., King, G., Spencer, C. & Scholz, C. 1982. The 1978 earthquake sequence near Thessaloniki (northern Greece). *Geophys. J. R. astr. Soc.* **68**, 429–458.

Stewart, J. H. 1980. Regional tilt patterns of late Cenozoic basin-range fault blocks, western United States. *Bull. geol. Soc. Am.* **91**, 460–464.

Stoneley, R. 1982. On the structural development of the Wessex basin. *J. geol. Soc. Lond.* **139**, 543–554.

Vening Meinesz, F. A. 1950. Les grabens africains, resultat de compression ou de tension dans le croute terrestre? *Inst. R. colonial Belge Bull.* **21**, 539–552.

Wallace, R. E. 1977. Profiles and ages of young fault scarps, north-central Nevada. *Bull. geol. Soc. Am.* **88**, 1267–1281.

Wallace, R. E. 1978. Geometry and rates of change of fault-generated range fronts, north-central Nevada. *J. Res. U.S. geol. Surv.* **6**, 637–650.

Wernicke, B. 1981. Low-angle normal faults in the Basin and Range Province: nappe tectonics in an extending orogen. *Nature, Lond.* **291**, 645–648.

Wernicke, B. & Burchfiel, B. C. 1982. Modes of extensional tectonics. *J. Struct. Geol.* **4**, 105–115.

Wood, R. 1982. Subsidence of the North Sea. Unpublished Ph.D. thesis, University of Cambridge.

Zandt, G. & Owens, T. J. 1980. Crustal flexure associated with normal faulting and implications for seismicity along the Wasatch Front, Utah. *Bull. seism. Soc. Am.* **70**, 1501–1520.

Zoback, M.-L., Anderson, R. E. & Thompson, G. A. 1981. Cainozoic evolution of the state of stress and style of tectonism of the Basin and Range province of the western United States. *Phil. Trans. R. Soc.* **A300**, 407–434.

APPENDIX 1

Dip variation due to pure shear

To determine the change in dip of a line drawn in a homogeneous fluid region extended by an amount β we need the 2×2 matrix **F** which converts an initial vector u' after deformation

$$u' = \mathbf{F}u. \tag{A1}$$

F is easily found by considering two special cases. When $u = (1, 0)$, a horizontal unit vector, the definition of β, the amount of extension, requires $u' = (\beta, 0)$. Similarly conservation of mass requires a vertical unit vector $(0, 1)$ to become $(0, 1/\beta)$. These two cases gives four equations for the four elements of **F**:

$$\mathbf{F} = \begin{pmatrix} \beta & 0 \\ 0 & \dfrac{1}{\beta} \end{pmatrix}. \tag{A2}$$

An initial unit vector at an angle θ to the horizontal $(\cos\theta, \sin\theta)$ is converted into a vector, which is no longer a unit vector, at an angle θ'_F to the horizontal. Combining (A1) and (A2) shows that

$$\tan\theta'_F = \frac{1}{\beta^2}\tan\theta. \tag{A3}$$

Equation (A3) is similar to equation (3.34) in Ramsay (1967), who describes the change of dip in terms of the axes of a strain ellipse, rather than in terms of β. The expression in (A3) does not allow for any contribution to β from motion on the line which deforms by pure shear.

APPENDIX 2

Vertical movement during faulting

If an isolated normal fault of dip θ cuts through a plate with an elastic thickness t_e, movement will produce uplift of the footwall and subsidence of the hanging wall. The easiest method of determining these movements is to consider the equilibrium of each side of the fault separately, and to imagine that each floats in a fluid whose density ρ_m is that of the mantle. We also suppose that the fault cuts through crust of density ρ_c and thickness t_c overlain by sediment of density ρ_s and of no strength. If we neglect the tilting of the fault, the total downwards force F_1 acting on the vertical section AA' through the end of the plate is (Fig. 8a):

$$F_1 = F + \frac{(\rho_c - \rho_s)gt_c^2}{2\tan\theta} - \left\{\frac{(\rho_m - \rho_s)g}{2\tan\theta} \times (t_c^2 - (t_c - t_m - w_1)^2)\right\} \tag{A4}$$

where F is the downwards force exerted by the hanging wall on the footwall, g is the acceleration due to gravity, w_1 is the displacement of the footwall and is measured downwards and

$$t_m = \frac{\rho_c - \rho_s}{\rho_m - \rho_s} t_c \tag{A5}$$

is the level which the mantle fluid would reach, measured from the base of the crust. If we assume $w_1 \ll t_m, t_c$

$$F_1 \simeq F - \frac{(\rho_m - \rho_s)g}{2 \tan \theta} (t_m + 2w_1)(t_c - t_m). \tag{A6}$$

Similarly the downward force F_2 on the vertical section BB' of the hanging wall, whose displacement is w_2, is (Fig. 8b):

$$\begin{aligned} F_2 &= -F + \frac{g(\rho_c - \rho_s)t_c^2}{2 \tan \theta} - g(\rho_m - \rho_s) \frac{(t_m + w_2)^2}{2 \tan \theta} \\ &\simeq -F + \frac{g(\rho_m - \rho_s)}{2 \tan \theta} t_m(t_c - t_m - 2w_2) \end{aligned} \tag{A7}$$

where $w_2 \ll t_m, t_c$ is the downward displacement of the hanging wall. As Heiskanen & Vening Meinesz (1958) show, the displacement w must satisfy

$$\frac{d^4 w}{dx^4} + \frac{4}{l^4} w = 0 \tag{A8}$$

where

$$l = \left(\frac{E t_e^3}{3g(\rho_m - \rho_s)(1 - \sigma^2)} \right)^{1/4} \tag{A9}$$

and has the dimensions of length, E is Young's modulus and σ Poisson's ratio. The flexural forces on the ends of each plate are related to the displacements through

$$F_1 = \frac{g(\rho_m - \rho_s)l}{2} w_1 \tag{A10}$$

and

$$F_2 = \frac{g(\rho_m - \rho_s)l}{2} w_2. \tag{A11}$$

If the ratio of footwall motion to hanging wall motion is f, then

$$w_1 = f w_2 \tag{A12}$$

substitution of (A10), (A11) and (A12) into (A6) and (A7), followed by addition, leads to an equation for f whose solution is

$$f = -\left(\frac{\rho_c - \rho_s + h}{\rho_m - \rho_c + h} \right) \tag{A13}$$

where

$$h = \frac{l \tan \theta (\rho_m - \rho_s)}{2t_c}. \tag{A14}$$

If the footwall is covered with water, rather than sediment, the ratio is approximately f_w where

$$f_w = \frac{\rho_c - \rho_s}{\rho_c - \rho_w} f \tag{A15}$$

where ρ_w is the density of water. If the footwall is subaerial, the ratio approximates to f_a where

$$f_a = \frac{\rho_c - \rho_s}{\rho_c} f. \tag{A16}$$

Substitution of $\rho_m = 3.3$ g cm^{-3}, $\rho_c = 2.8$ g cm^{-3}, $\rho_s = 2.5$ g cm^{-3}, and $\rho_w = 1.03$ g cm^{-3} gives

$$f_a = -0.06, \qquad f_w = -0.10$$

if $l = 0$ and

$$f_a = -0.08, \qquad f_w = -0.13$$

if $l = t_c$ and $\theta = 45°$. The negative sign of f indicates that the signs of w_1 and w_2 are different.

As (A13) shows, the ratio of the uplift to the subsidence is independent of the dip of the fault if the elastic thickness, and hence l, is zero. If the elastic thickness is not zero, h and f will increase with increasing θ. Hence the steeper second-generation faults will produce greater uplift of their footwalls than will the first-generation faults. Heiskanen & Vening Meinesz (1958) carried out a similar calculation but ignored the terms which depend on w_1 and w_2 in (A6) and (A7), respectively. The expressions in this Appendix are not exact, and in particular the effect of asymmetric loading is only approximated in (A15) and (A16). The purpose of these calculations is to estimate the ratio of footwall uplift to hanging-wall subsidence; which is about 10%. For a more elaborate discussion, involving more complex viscoelastic rheologies, the reader is referred to Zandt & Owens (1980).

Though the calculation above was motivated by observations of vertical movement during normal faulting, the sign of the fault displacement does not affect the result, which therefore applies equally to thrust faulting. As in the case of normal faulting, the expressions relating to asymmetric loading, (A15) and (A16), will only be approximate.